Rabi oscillation in few-photon double ionization through doubly excited states

Yinbo Chen,[1] Yueming Zhou,[1,*] Yang Li,[1] Min Li,[1] Pengfei Lan,[1] and Peixiang Lu[1,2,†]

[1]*School of Physics and Wuhan National Laboratory for Optoelectronics, Huazhong University of Science and Technology, Wuhan 430074, People's Republic of China*

[2]*Laboratory of Optical Information Technology, Wuhan Institute of Technology, Wuhan 430205, People's Republic of China*

(Received 31 October 2017; published 31 January 2018)

We theoretically investigate few-photon double ionization of helium in intense XUV laser fields by numerically solving the time-dependent Schrödinger equation. Our results show that the familiar single-ring structure in the joint electron momentum spectra is split into the double-ring and previously unobserved triple-ring structures at some specific photon energies. By tracing the electron population evolution of the corresponding states, we found that the triple-ring structure is induced by the coupled Rabi oscillations among the ground, a singly excited, and a doubly excited states. The intermediate detuning causes the asymmetry of the triple-ring structures, which can be controlled by changing the laser intensity and frequency.

DOI: 10.1103/PhysRevA.97.013428

I. INTRODUCTION

Electron correlation plays a vital role in the multielectron process of atoms or molecules, and has attracted considerable attention in the past decades [1–3]. As the simplest multielectron system, helium shows great superiority in exploring electron correlation and has been widely studied both in the energy [4,5] and time domain [6–8]. With the development of laser technologies, few-photon double ionization of He has been experimentally accessible and become a paradigm for studying the dynamics of electron correlations. Recently, the details of the electron correlations in few-photon double ionization of He have been well explored [9–11]. For example, it has been shown that two-photon double ionization (TPDI) occurs through two pathways, sequential and nonsequential TPDIs, depending on the photon energy of the laser fields. The electron correlation plays different roles in these pathways. In the sequential regime ($\hbar\omega > I_{p2}$, I_{p2} is the second ionization potential of He), the two electrons eject almost independently, while in the nonsequential regime ($\hbar\omega < I_{p2}$), the two electrons have to share energy to achieve double ionization. For ultrashort attosecond pulses, theoretical studies displayed that the electron correlations cannot be neglected even in the sequential TPDI regime, due to the attosecond temporal confinement of the emission of the two electrons [10–13]. Recently, numerous studies have performed to reveal and identify the detailed features of electron correlations in two- and few-photon double ionization [14–17].

Another important paradigm for studying correlated-electron dynamics is the doubly excited state (DES). Since the pioneering experiment [18] whose results are incompatible with the picture of two independent electrons, the electron correlation of DES has been extensively studied both experimentally and theoretically. Most of those studies are focused on the spectral domain [19–23]. Recently, investigation of the dynamics of DES in time domain with the ultrashort laser pulses has attracted increasing interest. For instance, it has been theoretically demonstrated that the correlated electron motion in the DES can be revealed by measuring the fully dimensional momentum spectra of the ejected electrons [6] or interference structures in the easily accessible single-electron spectra [24]. The process of few-photon double excitation of He has recently been experimentally traced with the free-electron laser fields [25] and the autoionization dynamics of the DES of He has been monitored using the attosecond pulses in the pump-probe experiment [8]. Very recently, the time evolution of the correlated electron wave packet in DES of He was reconstructed in the attosecond transient absorption spectra [26]. The buildup of the Fano profiles, which is the consequence of autoionization decay from DESs [27], is experimentally traced with the photoelectron spectroscopy [28] and extreme ultraviolet absorption spectroscopy [29]. These studies provide profound understanding on the dynamics of the correlated electrons in DESs.

In this paper, we theoretically study the correlated electron dynamics of DESs in few-photon double ionization by solving the reduced-dimensional time-dependent Schrödinger equation (TDSE). The results show that the joint electron momentum distributions from double ionization change from the single-ring to double-ring and a surprising triple-ring structures at some specific resonant photon energies. By checking the energy levels of the model atom and tracing the electron population evolution of the corresponding states, we identify that the double- and triple-ring structures are two kinds of Autler-Townes splitting [30–32]. The rapid Rabi oscillations among the ground state, a DES, and a singly excited state (SES) result in the Autler-Townes splitting of the involved states, leading to the double- and triple-ring structures in the momentum distributions. We mention that single-electron Rabi oscillation between the bound states has been observed and widely studied, both in strong-field single [33–37] and double ionizations [38]. However, the two-electron Rabi oscillation

*Corresponding author: zhouymhust@hust.edu.cn
†Corresponding author: lupeixiang@hust.edu.cn

involving DESs has been seldom observed. Our study predicts the strong correlated behaviors of the two-electron Rabi oscillation in few-photon double ionization.

II. NUMERICAL METHOD

The most accurate description of double ionization of He is numerically solving the full-dimensional TDSE. Though this has become accessible with the progress in the computing technology [7,11,14,39,40], the computation resource demand is huge. In the past years, numerous theoretical studies have resorted to the reduced (1+1)-dimensional model, where the two electrons are allowed to move along the laser polarization direction [41–43]. It has been shown that this reduced model can capture the main physics for the interaction of the two-electron system with strong-field laser with significantly reduced computational costs [43,44]. Therefore, in this work, we employ the (1+1)-dimensional model to study few-photon double ionization of He. In this model, the time evolution of the two-electron system in the laser field is obtained by numerically solving the equation (atomic units are used throughout until stated otherwise)

$$i\frac{\partial}{\partial t}\Phi(x_1,x_2,t) = H(x_1,x_2,t)\Phi(x_1,x_2,t). \tag{1}$$

Here $\Phi(x_1,x_2,t)$ is the time-dependent two-electron wave function and $H(x_1,x_2,t)$ is the corresponding Hamiltonian of the two-electron model He in the laser field. In the length gauge the Hamiltonian is written as

$$\begin{aligned} H(x_1,x_2,t) = &-\tfrac{1}{2}\left(\nabla_1^2+\nabla_2^2\right) + V_{ne}(x_1) + V_{ne}(x_2) \\ &+ V_{ee}(x_1,x_2) - (x_1+x_2)E(t), \end{aligned} \tag{2}$$

where the subscript $i = 1,2$ is the electron label. The potentials $V_{ne}(x_i) = -2/\sqrt{x_i^2+a^2}$ and $V_{ee}(x_1,x_2) = -2/\sqrt{(x_1-x_2)^2+b^2}$ represent the nuclear-electron and electron-electron interactions, respectively. The soft-core parameters $a = 0.707$ and $b = 0.582$ are chosen to reproduce the first ($I_{p1} = 0.90$ a.u.) and second ($I_{p2} = 2.00$ a.u.) ionization potentials of He [43]. $E(t)$ is the electric field of laser pulse with a total pulse duration of 30 fs. The laser pulses have a trapezoidal envelope which is switched on and off linearly over 3 fs, respectively. The bandwidth of the pulses is less than 0.005 a.u. This TDSE was solved with a split-operator spectral method [45,46] starting from the ground state of He obtained by the imaginary-time propagation method [47]. A large box size of 1600×1600 a.u. with the spatial step of 0.15 a.u. is used, and the time step in our calculations is 0.1 a.u. With a splitting technique [48–51], the two-electron wave function is smoothly split into the inner $\{|x_1| < s$ or $|x_2| < s\}$ and outer $\{|x_1|,|x_2| \geqslant s\}$ regions at time t_j with $s = 150$ a.u. We note that our results are insensitive to the choice of s ranging from 100 to 200 a.u. In the inner region, the wave function is propagated under the full Hamiltonian [Eq. (1)]. In the outer region the Coulomb interactions between the particles are neglected and the wave function is propagated under the Volkov Hamiltonian. Its evolution from t_j to the end of the laser pulse ($t \to \infty$) can be performed analytically in the momentum space

$$\begin{aligned} &\Phi_{o,p}(\infty;t_j) \\ &= \int \frac{\Phi_{o,r}(t_j)}{2\pi} e^{-i[p_1x_1+p_2x_2+A(t_j)(x_1+x_2)]}dx_1dx_2 \\ &\quad\times \exp\left\{-i\int_{t_j}^{\infty}\frac{[p_1+A(\tau)]^2+[p_2+A(\tau)]^2}{2}d\tau\right\}, \end{aligned} \tag{3}$$

where $A(t)$ is the vector potential of the laser pulse and $\Phi_{o,r}(t_j)$ is the wave function of the outer region in the coordinate space at t_j. The wave function near the outer edge of the total space box is absorbed with the masking function technique [52], so that the unphysical reflection and transmission are suppressed. After the end of the laser pulse, the wave functions are propagated freely for an additional 15 fs to get convergent results. Finally, the correlated momentum spectrum is given by

$$|\Phi_{o,p}(\infty)|^2 = |\Sigma_j\Phi_{o,p}(\infty,t_j)|^2. \tag{4}$$

III. RESULTS AND DISCUSSIONS

A. Joint electron momentum distributions

Figure 1 shows the joint electron momentum distributions for double ionization of the model He by 30 fs laser pulses with different frequencies. In Fig. 1(a), the photon energy is $\omega = 2.2$ a.u., higher than the sequential double-ionization threshold. Thus the two electrons could get ionized sequentially by absorbing one photon each. The momentum distribution shows the ring structure. The main distribution is clustered in distinct islands satisfying the emission of the first electron with energy of $\omega - I_{p1}$ and the second electron with the energy of $\omega - I_{p2}$. This is the typical distribution of the sequential TPDI [10,11,53]. In Fig. 1(a) there is also weak but visible distribution between these islands, which indicates nonsequential TPDI also occurs at photon energy higher than the second ionization potential. The joint momentum distribution provides much information about the details of the nonsequential ionization processes. For example, for the distribution in the first and third quadrants where the two electrons emit into the same direction, the nonsequential ionization signal exhibits a repulsion behavior along the diagonal $p_1 - p_2 = 0$. This indicates the effect of postionization interaction where Coulomb repulsion between the two simultaneously ionized electrons affects the final momentum distribution [12,53]. For the distribution in the second and fourth quadrants [Fig. 1(d)], the signal around the diagonal $p_1 + p_2 = 0$ indicates the mechanism of the second ionization during core relaxation in nonsequential ionization, where the second electron get ionized when the first electron still stays around the core and shares the dielectron interaction energy in the initial state [12]. Our results are consistent with previous studies at different photon energies in the sequential regime [11,53].

In Fig. 1(b), the photon energy is $\omega = 1.86$ a.u., lower than the second ionization potential. Thus TPDI could only occur through the nonsequential pathway. This is confirmed by the inner ring in the momentum distributions of Fig. 1(b) where the island structure disappears completely. In the first and third

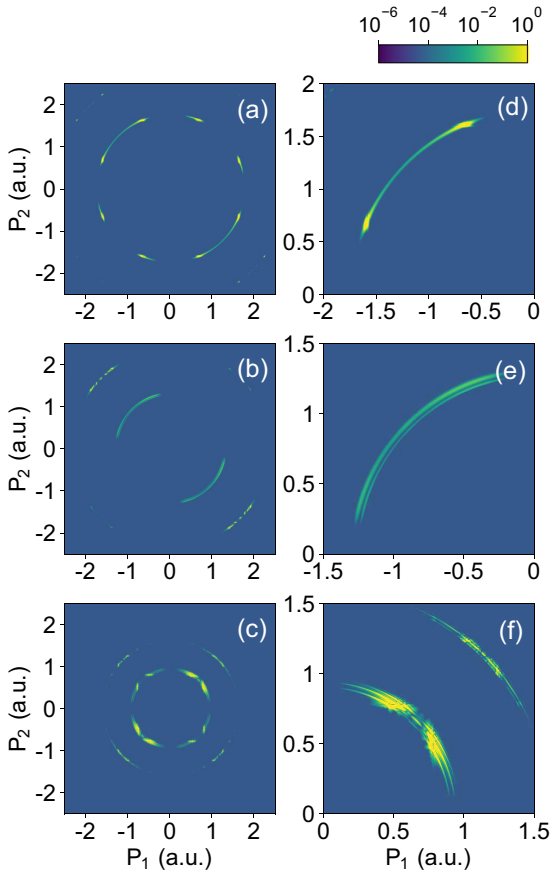

FIG. 1. Joint electron momentum for double ionization of He by XUV laser pulses with (a) $\omega = 2.2$ a.u., (b) $\omega = 1.86$ a.u., and (c) $\omega = 0.84$ a.u. The laser intensities are (a) and (b) $I = 5 \times 10^{16}$ W/cm^2 and (c) $I = 5 \times 10^{14}$ W/cm^2. Panels (d)–(f) respectively enlarge the distribution of (a)–(c) to highlight the single-ring, double-ring, and triple-ring structures. The pulse durations are 30 fs, respectively.

quadrants, the islands can be clearly seen in the outer ring, indicating the sequential process of the three-photon double ionization, i.e., the first and second electrons get ionized by respectively absorbing one and two photons. In the second and fourth quadrants, there is irregular structure in the three-photon double-ionization ring. This corresponds to the ionization process with shakeup [10,14,54], where He is first ionized to a series of excited He^+ states by absorbing two photons and then the excited He^+ is ionized by absorbing another photon. This process has been well explored in a recent study [55]. We return to the inner TPDI ring. For this ring, the distribution is well concentrated in the second and fourth quadrants, meaning that the two electrons prefer to emit into the opposite hemispheres in the nonsequential TPDI, in consistency with a previous experiment [56]. Closer inspection shows that this distribution exhibits a double-ring structure, as shown in Fig. 1(e). We mention that this double-ring structure has been observed in our previous studies on multiphoton above-threshold double ionization [42], where it was suggested that the double-ring structure originates from the Rabi oscillation between the ground and some DES of He. In the next subsection, we will explore the origin of this double-ring structure in nonsequential TPDI.

Figure 1(c) shows the electron momentum distribution for a lower photon energy of $\omega = 0.84$ a.u., where double ionization occurs by absorbing at least four photons. The first ring in Fig. 1(c) corresponds to the four-photon double ionization. There are two types of structure, the gridlike and the ring patterns. The gridlike pattern overlays the ring structure. By checking the position of this gridlike pattern, the four-photon double-ionization process can be determined, where the first electron is ionized leaving the second electron in the first excited state of He^+ (with the energy of -0.55 a.u. for our model He) by absorbing three photons and then the excited electron is subsequently ionized by absorbing another photon. This process leads to the final momenta of 0.53 a.u. and 0.76 a.u. for the first and second electrons, respectively. For the ring pattern, by zooming in the distribution in the first quadrant, a surprising triple-ring structure is observed. As we mentioned above, the double-ring structure was predicted in multiphoton above-threshold double ionization and it was identified as the Rabi oscillation of the electron pair in strong laser field [42]. Recently, Rabi oscillation of the single electron and electron pair in strong laser field has been experimentally observed [35,38,57]. This Rabi oscillation induces Autler-Townes splitting of the initial states and thus results in the double-ring structure in the momentum spectra for single [36] and double ionization [42]. However, the triple-ring structure has never been observed. In the following, we will focus on the underlying dynamics for this triple-ring structure.

B. Identify the double-ionization processes by checking the energy levels

To identify the double-ionization processes at different photon energies shown above, we calculate the bound-state energy levels of the model He using the autocorrelation function method [43,45,58]. To do this, we propagate an arbitrary initial wave packet $\psi(x_1,x_2,0)$ in the absence of laser field for a sufficiently long time and record the autocorrelation function $C(t) = \langle\psi(x_1,x_2,0)|\psi(x_1,x_2,t)\rangle$. Fourier transform of $C(t)$ yields the energies of all eigenstates in our model He atom [43]. In order to clarify the parity of the states, we choose the initial wave packet $\psi(x_1,x_2,0)$ as even and odd functions and separately calculate the autocorrelation function $C(t)$. Then, the energy levels with even and odd parities are obtained, as shown in Fig. 2. Here, the ground-state energy is set as $E_0 = 0$. Blue and purple lines represent the even- and odd-parity states, respectively. The SESs and DESs lie below and above the single-ionization threshold of $E = 0.90$ a.u. (indicated by the red solid vertical line). To check the accuracy of the autocorrelation function method in our calculation, we also have calculated the energy levels with the complex scaling method [59]. The results are well in agreement with the data in Fig. 2.

For simplicity, we label the two-electron states with the noninteracting electron symbol $|n_1,n_2\rangle$ [43,58]. $|1,1\rangle$ refers to the ground state of He. We pick up several relevant states in this study, $|1,1\rangle$, $|1,4\rangle$, $|2,2\rangle$, and $|2,3\rangle$, the energies of which are $E_0 = 0$, $E_1 = 0.84$ a.u., $E_2 = 1.67$ a.u., and $E_3 = 1.86$ a.u., respectively. According to the selection rules and the bandwidth of the laser pulse, the ground-state population can be transferred mainly to the DESs $|2,2\rangle$ and $|2,3\rangle$ by

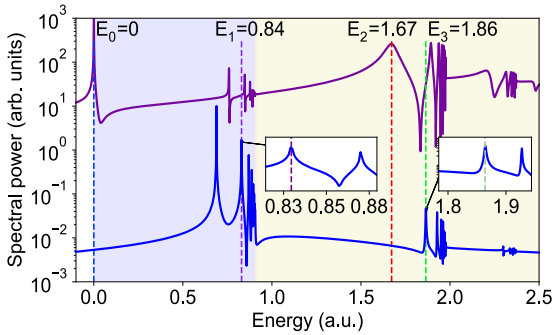

FIG. 2. Energy-levels diagram of the helium atom. The upper and the lower lines show all even- and odd-parity states, respectively. E_0, E_1, E_2, and E_3 are the energies of $|1,1\rangle$, $|1,4\rangle$, $|2,2\rangle$, and $|2,3\rangle$, respectively.

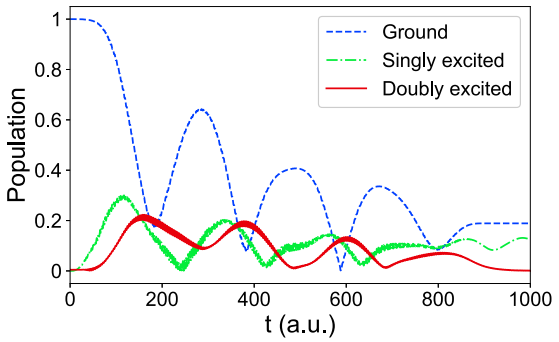

FIG. 3. Evolution of the population for the ground state $|1,1\rangle$, the SES $|1,5\rangle$, and the DES $|2,2\rangle$ in double ionization of He. The laser frequency and intensity are 0.84 a.u. and 5×10^{14} W/cm^2.

absorbing even and odd numbers of photons, respectively. Thus, for the photon energy $\omega = 1.86$ a.u., one-photon Rabi oscillation can occur between $|1,1\rangle$ and $|2,3\rangle$, which results in the Autler-Townes splitting of the ground-state energy level. Thus we can identify that the double-ring structure in Fig. 1(b) corresponds to the double ionization through the DES $|2,3\rangle$.

The photon energy of 0.84 a.u. in Fig. 1(c) exactly equals the energy difference of the singly excited state E_1 and the ground state E_0. Moreover, for this photon energy, the DES $|2,2\rangle$ is resonant with the ground state with two photons. It can be expected that the population transfer occurs between these states. Thus, at this photon energy, the double-ionization process occurs through several resonant intermediate states, within which multiple Rabi oscillations appear. This leads to the triple-ring structure in the electron momentum spectrum in Fig. 1(c), as will be explained in the next section.

C. Rabi oscillation and Autler-Townes splitting in few-photon double ionization

It is well known that Rabi oscillations between two bound states result in Autler-Townes splitting of the energy levels [30]. Thus doublet peaks appear in the energy spectrum of ionized electron when the photon energy is in resonance with the targets [42]. In our case, as shown above, three bound states are involved in resonance for the photon energy of 0.84 a.u. We employ a three-level model to show how the triplet structure appears. In the dressed-state picture, the three states $|a,N\rangle$, $|b,N-1\rangle$, and $|c,N-2\rangle$ are nearly degenerate, where $|a\rangle$, $|b\rangle$, and $|c\rangle$ stand for the ground state $|1,1\rangle$, singly excited state $|1,4\rangle$, and doubly excited state $|2,2\rangle$, respectively, and N is the photon number. In the laser field, the electric dipole interaction introduces coupling between these states. Following Ref. [60], we choose the energy of the initially uncoupled dressed states as zero. The Hamiltonian in the rotating-wave approximation is written as

$$H = \begin{bmatrix} 0 & \frac{1}{2}\Omega_{ab} & 0 \\ \frac{1}{2}\Omega_{ab} & \Delta & \frac{1}{2}\Omega_{bc} \\ 0 & \frac{1}{2}\Omega_{bc} & 0 \end{bmatrix}, \tag{5}$$

where Ω_{ab} and Ω_{bc} stand for the one-photon Rabi frequencies associated with the transition between $|1,1\rangle$ and $|1,4\rangle$, $|1,4\rangle$ and $|2,2\rangle$, respectively. Δ is the detuning of the intermediate state $|1,4\rangle$ with the laser frequency. By diagonalizing the Hamiltonian matrix, we have the cubic equation

$$E^3 - \Delta E^2 - \frac{E}{4}\left(\Omega_{ab}^2 + \Omega_{bc}^2\right) = 0. \tag{6}$$

Thus the eigenenergies are obtained,

$$E = 0, \tfrac{1}{2}\Delta \pm \tfrac{1}{2}\sqrt{\Delta^2 + \left(\Omega_{ab}^2 + \Omega_{bc}^2\right)}. \tag{7}$$

For small detuning, $\Delta \ll \Omega_1, \Omega_2$, the three eigenenergies are equally separated,

$$E = 0, \pm \tfrac{1}{2}\sqrt{\Omega_{ab}^2 + \Omega_{bc}^2}. \tag{8}$$

Thus, when coupled Rabi oscillations occur among these intermediate states during the ionization process, the splitting of the ground-state energy results in a triplet structure in the photoelectron spectrum [36], i.e., the triple-ring structure in the correlated electron momentum spectrum.

To confirm the coupled Rabi oscillations, we trace the population evolutions of these three states. To do this, we first calculate the involved eigenstates with the spectral method [45]. We employ a masking function to avoid the contribution of the singly ionized continuum. Then we trace the

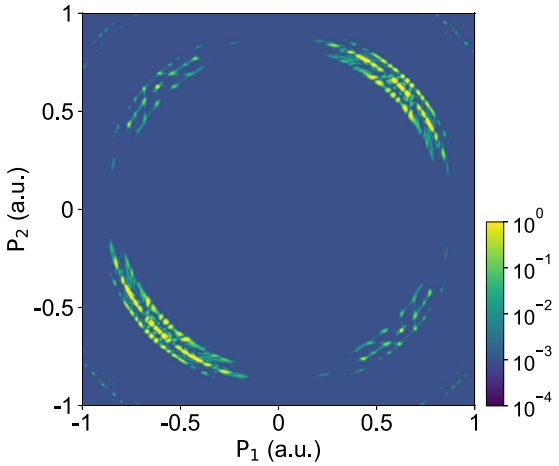

FIG. 4. Joint electron momentum distribution for double ionization of He by laser pulse with $\omega = 0.42$ a.u. The laser intensity is $I = 5 \times 10^{14}$ W/cm^2.

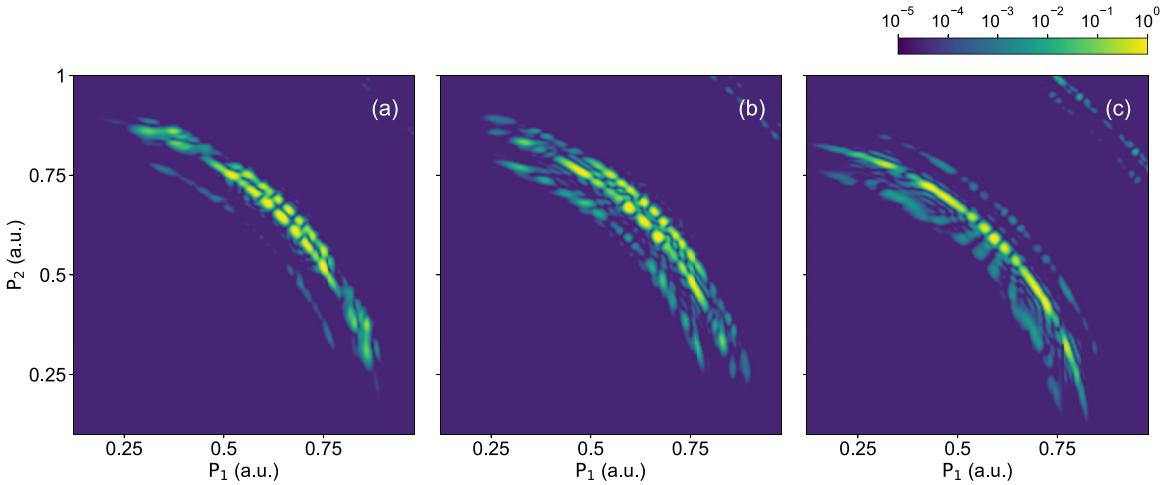

FIG. 5. Joint electron momentum distributions for double ionization of He by laser pulses with $\omega = 0.42$ a.u. The laser intensities are (a) 2×10^{14} W/cm^2, (b) 3.5×10^{14} W/cm^2, and (c) 10×10^{14} W/cm^2. The asymmetry parameters (see text) are 0.470, 0.089, and 0.008, respectively.

population evolution by projecting the wave function during the interaction with the laser field to these eigenstates at every t_j. Figure 3 shows the population's evolution of the involved ground, singly, and doubly excited states. The populations of these states oscillate at the frequency of 0.028 a.u., very close to the energy separation of the corresponding triple-ring structure in the joint momentum distribution of Fig. 1(c). With the three-level model, this Rabi frequency is calculated to be about 0.03 a.u. Figure 3 shows that the populations undergo over four oscillations before the laser field is turned off. This is sufficient for observation of the Autler-Townes splitting [31,34,61,62]. The damping of population oscillations results from depletion of the bound states due to the single and double ionization.

We also observe the effect of the coupled Rabi oscillations of the electron pair at other photon energies. Figure 4(a) shows the joint electron momentum distribution for double ionization at the photon energy of 0.42 a.u. The triple-ring structure is obvious. It is shown in Fig. 2 that there is a SES with even parity, the energy of which is about 0.84 a.u. above the ground state. Thus the electron could be resonantly excited to this state from the ground state by absorbing two photons. Also, the DES $|2,2\rangle$ could be occupied from this singly excited state through two-photon absorption. Thus the Rabi oscillations between these states occur, resulting in the triple-ring structure in the momentum spectrum.

We note that, in the real He, the energy levels of the excited states are very different from our 1D model. For example, the doubly excited state is higher than the sequential double-ionization threshold. Thus TPDI could occur sequentially at the resonance photon energy for double excitation and the double-ring structure will be less clear in TPDI. In this case, rather than the TPDI, one can observe the double-ring structure in few-photon double ionization where the sequential process is less prevalent. The triple-ring structure appearing in our 1D model benefits from the existence of an intermediate state which is simultaneously resonant with the ground and a doubly excited states. For real He, one could use two-color pulses with frequencies that are respectively resonant with the states. In this way the coupled Rabi oscillations involving three states occur and thus the triple-ring structure could appear.

In Fig. 5, we present momentum spectra for the photon energy of $\omega = 0.42$ a.u. at different intensities. It is shown that the energy separation in the triplet rings increases as the laser intensity increases. This is due to the fact that the Rabi frequencies increase with laser intensity. As shown in Eq. (7), the energy split increases accordingly. More obviously, the triplet-ring structure is asymmetric at the low laser intensity and becomes more symmetric at higher laser intensities. This results from the detuning effect. We quantify the detuning effect by defining an asymmetry parameter $A = \frac{||E_a - E_b| - |E_b - E_c||}{|E_a - E_b| + |E_b - E_c|}$, where E_a, E_b, E_c are the corresponding energies of peaks in the triplet-ring structure. With Eq. (7), we have $A = 1/\sqrt{1 + (\Omega_{ab}^2 + \Omega_{bc}^2)/\Delta^2}$. As the laser intensity increases, the Rabi frequencies increase and thus the parameter A becomes smaller ($A = 0$ indicates exactly symmetric triple-ring structure), i.e., the triple-ring structure becomes more symmetric.

IV. CONCLUSIONS

We have theoretically studied few-photon double ionization of He at different photon energies. The joint electron momentum distributions change from the familiar single-ring structure to the double-ring structure and previously unobserved triple-ring structure at some specific photon energies. By checking the energy levels of the model atom, we have identified that the double-ring structure results from the Rabi oscillation between the ground and a doubly excited state during laser pulse. For the triple-ring structure, coupled Rabi oscillations of the electron pair between the ground state, a singly excited state, and a doubly excited states occur, which are confirmed by tracing the population transfer. These coupled Rabi oscillations result in the triple splitting of the involved bound-state energy levels, leading to the triple-ring structure in the electron momentum

distribution. The triple-ring structure is also observed at other photon energy where the coupled Rabi oscillations between three bound states are allowed. We also studied the dependence of this structure on the laser intensity. It indicates that the correlated behavior of the electron pair can be controlled by the laser intensity.

ACKNOWLEDGMENTS

This work was supported by National Natural Science Foundation of China (Grants No. 11622431, No. 11604108, No. 11627809, and No. 61475055) and Program for HUST Academic Frontier Youth Team.

[1] W. Becker, X. Liu, P. J. Ho, and J. H. Eberly, Rev. Mod. Phys. **84**, 1011 (2012).
[2] G. Tanner, K. Richter, and J. M. Rost, Rev. Mod. Phys. **72**, 497 (2000).
[3] M. Ossiander, F. Siegrist, V. Shirvanyan, R. Pazourek, A. Sommer, T. Latka, A. Guggenmos, S. Nagele, J. Feist, J. Burgdörfer, R. Kienberger, and M. Schultze, Nat. Phys. **13**, 280 (2016).
[4] R. Moshammer, J. Ullrich, M. Unverzagt, W. Schmidt, P. Jardin, R. E. Olson, R. Mann, R. Dörner, V. Mergel, U. Buck, and H. Schmidt-Böcking, Phys. Rev. Lett. **73**, 3371 (1994).
[5] L. H. Andersen, P. Hvelplund, H. Knudsen, S. P. Møller, J. O. P. Pedersen, S. Tang-Petersen, E. Uggerhøj, K. Elsener, and E. Morenzoni, Phys. Rev. A **41**, 6536 (1990).
[6] T. Morishita, S. Watanabe, and C. D. Lin, Phys. Rev. Lett. **98**, 083003 (2007).
[7] S. X. Hu and L. A. Collins, Phys. Rev. Lett. **96**, 073004 (2006).
[8] S. Gilbertson, M. Chini, X. Feng, S. Khan, Y. Wu, and Z. Chang, Phys. Rev. Lett. **105**, 263003 (2010).
[9] L. Y. Peng, Z. Zhang, W. C. Jiang, G. Q. Zhang, and Q. Gong, Phys. Rev. A **86**, 063401 (2012).
[10] J. Feist, R. Pazourek, S. Nagele, E. Persson, B. I. Schneider, L. A. Collins, and J. Burgdörfer, J. Phys. B **42**, 134014 (2009).
[11] J. Feist, S. Nagele, R. Pazourek, E. Persson, B. I. Schneider, L. A. Collins, and J. Burgdörfer, Phys. Rev. Lett. **103**, 063002 (2009).
[12] K. L. Ishikawa and K. Midorikawa, Phys. Rev. A **72**, 013407 (2005).
[13] E. Foumouo, P. Antoine, H. Bachau, and B. Piraux, New J. Phys. **10**, 025017 (2008).
[14] R. Pazourek, J. Feist, S. Nagele, E. Persson, B. I. Schneider, L. A. Collins, and J. Burgdörfer, Phys. Rev. A **83**, 053418 (2011).
[15] S. Selstø, X. Raynaud, A. S. Simonsen, and M. Førre, Phys. Rev. A **90**, 053412 (2014).
[16] W. C. Jiang, J. Y. Shan, Q. Gong, and L. Y. Peng, Phys. Rev. Lett. **115**, 153002 (2015).
[17] A. Liu and U. Thumm, Phys. Rev. Lett. **115**, 183002 (2015).
[18] R. P. Madden and K. Codling, Phys. Rev. Lett. **10**, 516 (1963).
[19] M. Domke, G. Remmers, and G. Kaindl, Phys. Rev. Lett. **69**, 1171 (1992).
[20] J. Z. Tang, S. Watanabe, and M. Matsuzawa, Phys. Rev. A **48**, 841 (1993).
[21] Y. K. Ho, Phys. Rev. A **34**, 4402 (1986).
[22] M. Domke, K. Schulz, G. Remmers, G. Kaindl, and D. Wintgen, Phys. Rev. A **53**, 1424 (1996).
[23] K. Schulz, G. Kaindl, M. Domke, J. D. Bozek, P. A. Heimann, A. S. Schlachter, and J. M. Rost, Phys. Rev. Lett. **77**, 3086 (1996).
[24] J. Feist, S. Nagele, C. Ticknor, B. I. Schneider, L. A. Collins, and J. Burgdörfer, Phys. Rev. Lett. **107**, 093005 (2011).
[25] A. Hishikawa, M. Fushitani, Y. Hikosaka, A. Matsuda, C. N. Liu, T. Morishita, E. Shigemasa, M. Nagasono, K. Tono, T. Togashi, H. Ohashi, H. Kimura, Y. Senba, M. Yabashi, and T. Ishikawa, Phys. Rev. Lett. **107**, 243003 (2011).
[26] C. Ott, A. Kaldun, L. Argenti, P. Raith, K. Meyer, M. Laux, Y. Zhang, A. Blättermann, S. Hagstotz, T. Ding, R. Heck, J. Madroñero, F. Martín, and T. Pfeifer, Nature (London) **516**, 374 (2014).
[27] U. Fano, Phys. Rev. **124**, 1866 (1961).
[28] V. Gruson, L. Barreau, A. Jimenez-Galan, F. Risoud, J. Caillat, A. Maquet, B. Carre, F. Lepetit, J.-F. Hergott, T. Ruchon, L. Argenti, R. Taieb, F. Martin, and P. Salieres, Science **354**, 734 (2016).
[29] A. Kaldun, A. Blattermann, V. Stooss, S. Donsa, H. Wei, R. Pazourek, S. Nagele, C. Ott, C. D. Lin, J. Burgdorfer, and T. Pfeifer, Science **354**, 738 (2016).
[30] S. H. Autler and C. H. Townes, Phys. Rev. **100**, 703 (1955).
[31] B. Walker, M. Kaluža, B. Sheehy, P. Agostini, and L. F. DiMauro, Phys. Rev. Lett. **75**, 633 (1995).
[32] U. Lambrecht, M. Nurhuda, and F. H. M. Faisal, Phys. Rev. A **57**, R3176 (1998).
[33] Z. Sun and N. Lou, Phys. Rev. Lett. **91**, 023002 (2003).
[34] M. Wollenhaupt, A. Assion, O. Bazhan, C. Horn, D. Liese, C. Sarpe-Tudoran, M. Winter, and T. Baumert, Phys. Rev. A **68**, 015401 (2003).
[35] M. Fushitani, C. N. Liu, A. Matsuda, T. Endo, Y. Toida, M. Nagasono, T. Togashi, M. Yabashi, T. Ishikawa, Y. Hikosaka, T. Morishita, and A. Hishikawa, Nat. Photon. **10**, 102 (2015).
[36] K. J. Yuan, Z. Sun, S. L. Cong, and N. Lou, Phys. Rev. A **74**, 043421 (2006).
[37] T. Sako, J. Adachi, A. Yagishita, M. Yabashi, T. Tanaka, M. Nagasono, and T. Ishikawa, Phys. Rev. A **84**, 053419 (2011).
[38] M. Flögel, J. Durá, B. Schütte, M. Ivanov, A. Rouzée, and M. J. J. Vrakking, Phys. Rev. A **95**, 021401(R) (2017).
[39] Z. Zhang, L. Y. Peng, M. H. Xu, A. F. Starace, T. Morishita, and Q. Gong, Phys. Rev. A **84**, 043409 (2011).
[40] J. M. Ngoko Djiokap, N. L. Manakov, A. V. Meremianin, S. X. Hu, L. B. Madsen, and A. F. Starace, Phys. Rev. Lett. **113**, 223002 (2014).
[41] M. Lein, E. K. U. Gross, and V. Engel, Phys. Rev. Lett. **85**, 4707 (2000).
[42] Q. Liao, Y. M. Zhou, C. Huang, and P. X. Lu, New J. Phys. **14**, 013001 (2012).
[43] Z. Q. Yang, D. F. Ye, T. Ding, T. Pfeifer, and L. B. Fu, Phys. Rev. A **91**, 013414 (2015).
[44] M. Lein, E. K. U. Gross, and V. Engel, Phys. Rev. A **64**, 023406 (2001).
[45] M. D. Feit and J. A. Fleck, J. Chem. Phys. **78**, 301 (1983).
[46] R. Heather and H. Metiu, J. Chem. Phys. **86**, 5009 (1987).

[47] R. Kosloff and H. Tal-Ezer, Chem. Phys. Lett. **127**, 223 (1986).
[48] X. M. Tong, K. Hino, and N. Toshima, Phys. Rev. A **74**, 031405 (2006).
[49] Y. Li, M. Li, Y. Zhou, X. Ma, H. Xie, P. Lan, and P. Lu, Opt. Express **25**, 11233 (2017).
[50] S. A. Rezvani, Z. Hong, X. Pang, S. Wu, Q. Zhang, and P. Lu, Opt. Lett. **42**, 3367 (2017); X. Liu, X. Zhu, P. Lan, X. Zhang, D. Wang, Q. Zhang, and P. Lu, Phys. Rev. A **95**, 063419 (2017).
[51] X. Ma, M. Li, Y. Zhou, and P. Lu, Opt. Quantum Electron. **49**, 170 (2017); M. He, Y. Li, Y. Zhou, M. Li, and P. Lu, Phys. Rev. A **93**, 033406 (2016); M. He, Y. Zhou, Y. Li, M. Li, and P. Lu, Opt. Quantum Electron. **49**, 232 (2017); J. Tan, Y. Li, Y. M. Zhou, M. R. He, Y. B. Chen, M. Li, and P. X. Lu, *ibid.* **50**, 57 (2018).
[52] F. He, C. Ruiz, and A. Becker, Phys. Rev. A **75**, 053407 (2007).
[53] Z. Zhang, L. Y. Peng, Q. Gong, and T. Morishita, Opt. Express **18**, 8976 (2010).
[54] R. Pazourek, J. Feist, S. Nagele, and J. Burgdörfer, Phys. Rev. Lett. **108**, 163001 (2012).
[55] C. Yu and L. B. Madsen, Phys. Rev. A **93**, 043412 (2016).
[56] A. Rudenko *et al.*, Phys. Rev. Lett. **101**, 073003 (2008).
[57] S. Zhdanovich, J. W. Hepburn, and V. Milner, Phys. Rev. A **84**, 053428 (2011).
[58] J. Zhao and M. Lein, New J. Phys. **14**, 065003 (2012).
[59] A. Cerioni, L. Genovese, I. Duchemin, and T. Deutsch, J. Chem. Phys. **138**, 204111 (2013).
[60] A. F. Linskens, I. Holleman, N. Dam, and J. Reuss, Phys. Rev. A **54**, 4854 (1996).
[61] S. E. Moody and M. Lambropoulos, Phys. Rev. A **15**, 1497 (1977).
[62] M. A. Quesada, A. M. F. Lau, D. H. Parker, and D. W. Chandler, Phys. Rev. A **36**, 4107 (1987).